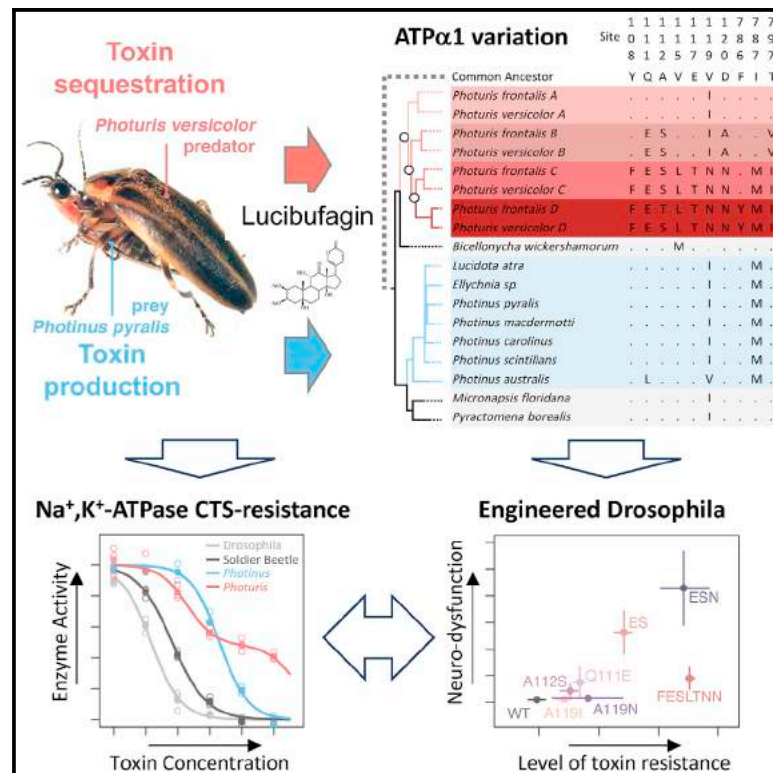


# Current Biology

## Predatory fireflies and their toxic firefly prey have evolved distinct toxin resistance strategies

### Graphical abstract



### Authors

Lu Yang, Flora Borne, Anja Betz, ...,  
Michael J. Palladino,  
Georg Petschenka, Peter Andolfatto

### Correspondence

pa2543@columbia.edu

### In brief

Animal species that obtain defensive toxins from their diet are likely to face distinct physiological challenges from species that synthesize toxins internally. Yang et al. reveal that fireflies that produce toxins internally and fireflies that have specialized to predate them have evolved toxin-resistant Na<sup>+</sup>,K<sup>+</sup>-ATPases via distinct mechanisms.

### Highlights

- To obtain defensive lucibufagin toxins, *Photuris* fireflies predate other fireflies
- *Photuris* have evolved ATP $\alpha$ 1 paralogs with increasing levels of toxin resistance
- Firefly genera that synthesize toxins internally retain a single resistant ATP $\alpha$ 1
- *Drosophila* engineering reveals major determinants of toxin resistance in fireflies



## Article

# Predatory fireflies and their toxic firefly prey have evolved distinct toxin resistance strategies

Lu Yang,<sup>1</sup> Flora Borne,<sup>2</sup> Anja Betz,<sup>3</sup> Matthew L. Aardema,<sup>1,4</sup> Ying Zhen,<sup>1,5</sup> Julie Peng,<sup>1</sup> Regina Visconti,<sup>1</sup> Mariana Wu,<sup>1</sup> Bartholomew P. Roland,<sup>6,7</sup> Aaron D. Talsma,<sup>6,7</sup> Michael J. Palladino,<sup>6,7</sup> Georg Petschenka,<sup>3</sup> and Peter Andolfatto<sup>2,8,9,\*</sup>

<sup>1</sup>Department of Ecology and Evolutionary Biology, Princeton University, Princeton, NJ 08544, USA

<sup>2</sup>Department of Biological Sciences, Columbia University, New York, NY 10027, USA

<sup>3</sup>Department of Applied Entomology, University of Hohenheim, 70599 Stuttgart, Germany

<sup>4</sup>Department of Biology, Montclair State University, Montclair, NJ 07043, USA

<sup>5</sup>School of Life Sciences, Westlake University, Hangzhou 310024, China

<sup>6</sup>Department of Pharmacology and Chemical Biology, University of Pittsburgh, Pittsburgh, PA 15261, USA

<sup>7</sup>Pittsburgh Institute for Neurodegenerative Diseases, University of Pittsburgh School of Medicine, Pittsburgh, PA 15261, USA

<sup>8</sup>X (formerly Twitter): @pandolfatto

<sup>9</sup>Lead contact

\*Correspondence: pa2543@columbia.edu

<https://doi.org/10.1016/j.cub.2023.10.063>

## SUMMARY

Toxic cardiotoxic steroids (CTSs) act as a defense mechanism in many firefly species (Lampyridae) by inhibiting a crucial enzyme called Na<sup>+</sup>,K<sup>+</sup>-ATPase (NKA). Although most fireflies produce these toxins internally, species of the genus *Photuris* acquire them from a surprising source: predation on other fireflies. The contrasting physiology of toxin exposure and sequestration between *Photuris* and other firefly genera suggests that distinct strategies may be required to prevent self-intoxication. Our study demonstrates that both *Photuris* and their firefly prey have evolved highly resistant NKAs. Using an evolutionary analysis of the specific target of CTS (ATP $\alpha$ ) in fireflies and gene editing in *Drosophila*, we find that the initial steps toward resistance were shared among *Photuris* and other firefly lineages. However, the *Photuris* lineage subsequently underwent multiple rounds of gene duplication and neofunctionalization, resulting in the development of ATP $\alpha$  paralogs that are differentially expressed and exhibit increasing resistance to CTS. By contrast, other firefly species have maintained a single copy. Our results implicate gene duplication as a facilitator in the transition of *Photuris* to its distinct ecological role as a predator of toxic firefly prey.

## INTRODUCTION

Many species of fireflies (family Lampyridae, subfamily Lampyrinae) produce a class of defensive toxins called cardiotoxic steroids (CTSs) that they use to deter potential predators.<sup>1–6</sup> By contrast, fireflies in the genus *Photuris* (family Lampyridae, subfamily Photurinae) cannot manufacture their own CTSs. Instead, they acquire these toxins by preying on CTS-producing firefly species, using them as a defense for both themselves and their eggs (Figure 1A).<sup>7–9</sup> Although most Lampyridae are predatory, only *Photuris* is documented to frequently prey on other fireflies. Among other adaptations associated with this specialization,<sup>10</sup> female *Photuris* mimic the courtship signals of other female Lampyridae (including congeners) to attract male prey, earning them the moniker “*femmes fatales*.”<sup>7,11</sup>

CTSs act by inhibiting Na<sup>+</sup>,K<sup>+</sup>-ATPase (NKA), an essential enzyme that helps maintain homeostasis in animals.<sup>12,13</sup> CTS-resistant forms of NKA have evolved repeatedly across diverse insects and vertebrates via amino acid substitutions to the CTS-binding domain of the enzyme’s alpha-subunit (ATP $\alpha$ , more specifically ATP $\alpha$ 1).<sup>14–22</sup> CTS adaptation in insects exhibits two distinct recurrent patterns of ATP $\alpha$  molecular evolution. The first is that CTS resistance typically evolves via a small number of

amino acid changes and most frequently via substitutions to three sites (111, 119, and 122) in the first extracellular domain (H1-H2) of the protein.<sup>14,15,22–24</sup> A second recurrent pattern in CTS-adapted insects is the frequent duplication and neofunctionalization of ATP $\alpha$ , with resistant and sensitive paralogs differentially allocated to the gut and nervous tissue.<sup>21,22,25</sup> These findings generally point to a high degree of predictability in the genetic basis of CTS-resistance evolution in insects.<sup>21,22</sup>

Here, we investigate whether ATP $\alpha$ 1 is also a target of CTS adaptation in fireflies and whether these adaptations evolved via similar mechanisms in firefly predators (i.e., *Photuris*) and other firefly lineages. *Photuris* species share a number of adaptations with other fireflies including warning coloration and bioluminescent signaling (with associated structures). Collectively, these similarities likely reflect a combination of shared history and convergent evolution.<sup>26–29</sup> Accordingly, it is also possible that CTS resistance in *Photuris* and other firefly species evolved either in their common ancestor or convergently via similar molecular mechanisms. Alternatively, given the different physiological challenges associated with sequestering these toxins from a food source (i.e., *Photuris*) versus producing CTS autogenously (i.e., most other firefly species),<sup>30–32</sup> it is also possible that distinct modes of CTS resistance evolved independently in *Photuris* and other firefly lineages.



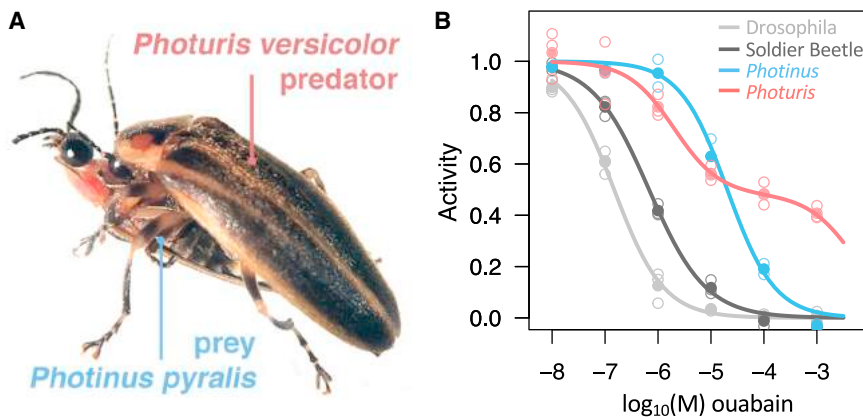


**Figure 1.  $\text{Na}^+/\text{K}^+$ -ATPase (NKA) resistance to cardiotoxic steroids (CTSs) in predatory and prey firefly species**

(A) Female *Photuris versicolor* preying on a *Photinus pyralis* male (photo by L.Y., 2017).

(B) CTS-inhibition assay on firefly brain and ventral nerve cord NKA shows that both *Photuris versicolor* (red) and *Photinus pyralis* (blue) are relatively resistant to ouabain (a representative CTS). Mean relative ATPase activity of NKA (closed circles) is plotted as a function of increasing molar (M) concentrations of the CTS ouabain. Open circles indicate biological replicates ( $n = 3$  for all except *Photinus*,  $n = 2$ ). The NKA of both fireflies is significantly more resistant than that of the Red Soldier Beetle (*Rhagonycha fulva*) and *Drosophila* (*D. melanogaster* w1118) (Table S4). The fitted

curves for *Drosophila*, Red Soldier Beetle, and *Photinus pyralis* assume monophasic inhibition functions, whereas that for *Photuris versicolor* is assumed to be biphasic (STAR Methods).

## RESULTS

### Duplication and neofunctionalization of $\text{ATP}\alpha 1$ in *Photuris*

To investigate the basis of CTS resistance in predator and prey firefly species, we first considered the level of CTS resistance of membrane-bound NKA proteins isolated from the nervous systems of wild-caught *Photinus pyralis* (a representative CTS-producing prey species) and *Photuris versicolor* (a representative predator species) and compared these to the closely related Red Soldier Beetle (*Rhagonycha fulva*) as well as *Drosophila* (*Drosophila melanogaster*). The NKA of both firefly species exhibits substantially higher resistance to ouabain—a water-soluble CTS—than both the Red Soldier Beetle and *Drosophila* enzymes (Figure 1B; Table S4). Although the monophasic inhibition curves for *Drosophila*, the Red Soldier Beetle, and *Photinus* suggest a single resistant form of the enzyme, the curve for *Photuris* is still only partially inhibited at the highest inhibitor concentrations. We hypothesized that the curve is likely to be a truncated biphasic (or multi-phasic) curve, indicating that *Photuris* may have multiple isoforms of NKA that differ in their level of CTS resistance. Notably, despite having no exposure to CTSs, the NKA of the Red Soldier Beetle is 4.6-fold more resistant to CTS than the *Drosophila* protein (Figure 1B; Table S4).

Using RNA sequencing (RNA-seq) *de novo* assembly and available *de novo* genome assemblies (Table S1), we reconstructed  $\text{ATP}\alpha 1$  sequences for multiple firefly species and outgroups. Consistent with our *in vitro* CTS-inhibition assays (above), we found that the Red Soldier Beetle, *Photinus*, and other toxin-producing firefly genera appear to have a single copy of  $\text{ATP}\alpha 1$ . By contrast, both *Photuris* species surveyed harbor multiple copies of  $\text{ATP}\alpha 1$  that we designate as paralogs A–D (Figure 2A). Our analysis of RNA-seq data indicates that duplications of  $\text{ATP}\alpha 1$  are also absent or not expressed in *Bicellonycha*, an outgroup to the *Photuris* genus (STAR Methods). Together with the phylogenetic tree (Figure 2), this evidence suggests that all three duplication events occurred after the split of *Photuris* and *Bicellonycha* (~50 mya<sup>33</sup>), but prior to the split between *Photuris versicolor* and *Photuris frontalis*. Given the ages of these duplications relative to the *P. versicolor* and *P. frontalis*

divergence<sup>33,34</sup> (Figure 2A), it is likely that they are shared by most, if not all, species of the *Photuris* genus.

*Photuris*  $\text{ATP}\alpha 1$  paralogs are differentially expressed among tissues. Based on the pattern of amino acid substitution at sites previously implicated in CTS resistance,  $\text{ATP}\alpha 1A$  is predicted to be the most CTS-sensitive paralog and is more highly expressed in head relative to gut tissue (adjusted  $p = 3.0e-6$ ). Conversely,  $\text{ATP}\alpha 1C$  and  $\text{ATP}\alpha 1D$  are predicted to be the most CTS-resistant paralogs because they have accumulated multiple amino acid substitutions implicated in CTS resistance (Figures 2A and 2B). In contrast to  $\text{ATP}\alpha 1A$ ,  $\text{ATP}\alpha 1C$  is substantially more highly expressed in the gut relative to the head (adjusted  $p = 8.8e-4$ ; Table S2; Figure 2C). This implies that  $\text{ATP}\alpha 1$  paralogs have neofunctionalized, as observed in multiple CTS-adapted insects carrying  $\text{ATP}\alpha 1$  duplications.<sup>21,22,25</sup>  $\text{ATP}\alpha 1A$  and  $\text{ATP}\alpha 1C$  together comprise 88% of  $\text{ATP}\alpha 1$  transcripts in the female *Photuris* head and are represented in roughly equal proportions (Figure 2C), lending support to the “biphasic” interpretation of the enzyme-inhibition curve for *Photuris* nervous tissue (Figure 1B). Given the stepwise accumulation of amino acid substitutions among *Photuris* paralogs (Figure 2B), we used CRISPR-Cas9 genome editing (STAR Methods), and a similar site-directed cassette exchange system,<sup>23</sup> to generate a series of *Drosophila melanogaster* strains that carry substitutions occurring at key stages of  $\text{ATP}\alpha 1$  neofunctionalization in *Photuris* (Figure 3A).

### Stepwise accumulation of CTS-resistance substitutions in firefly lineages

Phylogenetic inference reveals that the first steps in the evolution of  $\text{ATP}\alpha 1$  CTS resistance were shared between *Photuris* and other firefly lineages. Specifically, the substitution of alanine to valine at position 119 (A119V) likely preceded the origin of fireflies (Figures 2B and S1). The higher CTS resistance of Red Soldier Beetle NKA relative to *Drosophila* (Figure 1B) is consistent with a contribution of this substitution to NKA CTS resistance. A subsequent substitution to the same site, V119I, is observed in both *Photuris* and other firefly species. *Bicellonycha* is a member of a sister genus to *Photuris*,<sup>33</sup> and the species we surveyed (*B. wickershamorum*) lacks V119I. In fact, our phylogenetic analysis suggests that *Bicellonycha* retains the ancestral state and that V119I most likely evolved convergently in both

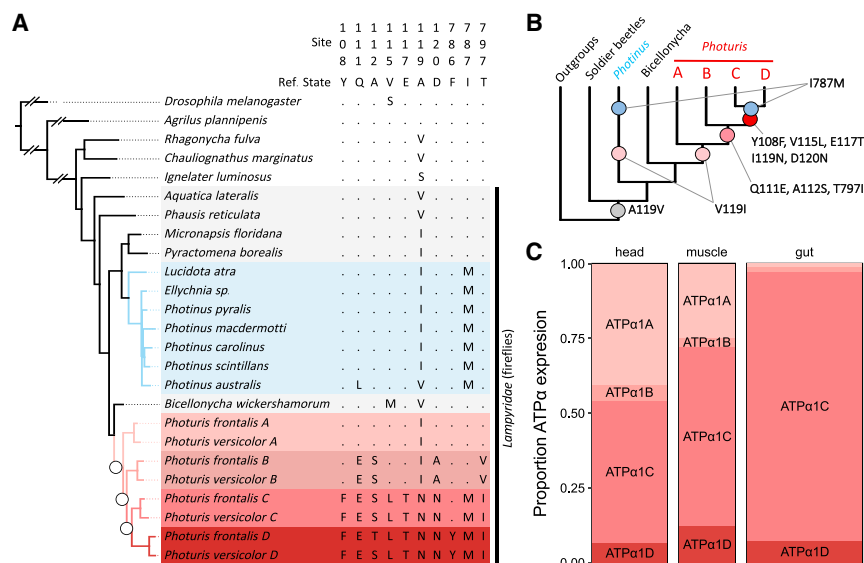


**Figure 2. Molecular evolution of ATP $\alpha$ 1 in fireflies**

(A) A maximum likelihood genealogical tree based on ATP $\alpha$ 1 protein-coding sequences (see STAR Methods, Table S1, and Figure S1 for more details). All species are beetles (Coleoptera), except for *Drosophila melanogaster*. CTS-producing firefly species are shaded in blue, and four *Photuris* ATP $\alpha$ 1 paralog lineages A–D are indicated in increasingly darker shades of red. White circles indicate three sequential rounds of duplication in the *Photuris* lineage. Substitution patterns are shown only for sites with known roles in CTS resistance, except for site 787, which is newly discovered in this study. The reference sequence corresponds to the reconstructed ancestral sequence for beetles. Dots indicate identity with the ancestral state, and letters represent derived amino acid substitutions. The phylogenetic position of *Bicellonycha wickershamorum* has 86% bootstrap support and is consistent with phylogenetic reconstructions based on multiple loci.<sup>33,35</sup>

(B) Schematic graph showing key amino acid substitutions inferred to have occurred in species and paralog lineages. Soldier beetles are represented by *Rhagonycha* and *Chauliognathus*. See Figure S1 for more details.

(C) Tissue-specific expression of ATP $\alpha$ 1 paralogs in *Photuris versicolor* females (Table S2; Figure S2). Column width corresponds to relative proportion of total normalized ATP $\alpha$ 1 expression summed across paralogs in *Photuris*, and shaded segments correspond to the relative levels of expression of the four ATP $\alpha$ 1 paralogs in each tissue.

*Photuris* and other firefly species soon after they became distinct lineages (Figures 2B and S1).

To estimate the functional effects of the eventual transition from alanine to isoleucine at position 119 in *Photuris* and other firefly lineages (i.e., A119I = 119A  $\rightarrow$  119V  $\rightarrow$  119I), we modified the *D. melanogaster* ATP $\alpha$ 1 protein using genome-editing tools. We find that A119I modestly but significantly increases CTS resistance of NKA relative to the sensitive wild-type *D. melanogaster* enzyme (1.8-fold, 95% confidence interval [CI]: 1.6–1.9; Figure 3B). A119I also substantially improves *D. melanogaster* adult survival upon exposure to CTSs (Figure 3C). Since NKA is critical for proper neural function, we subjected adult engineered flies to mechanical over-stimulation and measured recovery time from induced seizures (the so-called bang sensitivity assay<sup>36</sup>; STAR Methods). We found that A119I mutant flies exhibit no obvious neurological dysfunction compared with wild-type flies (Figure 3D). Taken together, we conclude that the evolution of alanine to isoleucine at position 119 comprises a potential exaptation that may have facilitated the emergence of both the ability of fireflies to manufacture CTSs and the predatory specialization of *Photuris*.

Despite these shared early steps in the evolution ATP $\alpha$ 1 CTS resistance, it is apparent that lineages leading to the predatory genus *Photuris* subsequently took a radically different approach compared with other fireflies: repeated duplication and neofunctionalization of ATP $\alpha$ 1. Following an initial duplication of ATP $\alpha$ 1 in the *Photuris* lineage, two paralogous lineages began to diverge in function, with one lineage ancestral to more resistant paralogs B–D. The most conspicuous candidate CTS-resistance substitutions on the B–D lineage are Q111E and T797I (Figure 2B). Site 111 is a known hotspot for convergent CTS-resistance substitutions in animals.<sup>14,17,22</sup> At site 797, the ancestral threonine residue is predicted to form a stabilizing hydrogen bond between ATP $\alpha$ 1 and CTSs<sup>37</sup> that the derived T797I

substitution (along the paralog B–D lineage) is predicted to disrupt. Previous work established that the biochemically similar substitution T797V results in an 80-fold increase in CTS resistance of mammalian NKA.<sup>38</sup> A substitution to a third site in the paralog B–D lineage, A112S, was also of interest as this site was previously identified as a target of positive selection in CTS-resistant toads and their predators.<sup>18</sup> Further, A112S repeatedly co-occurs with Q111E/R/T across phylogenetically diverse taxa including both insects and vertebrates.<sup>17,23</sup>

Given these substitution patterns, we engineered a series of *D. melanogaster* lines to dissect the basis for CTS resistance along the lineage leading to paralogs B–D. We began by focusing on substitutions at sites 111 and 112. NKA isolated from fly lines engineered with Q111E + A112S (hereafter “ES”) exhibits a 6-fold increase in CTS resistance relative to the wild-type enzyme of *Drosophila* (Figure 3B; Table S4). Together, these substitutions also confer engineered adult flies with substantial levels of resistance to CTS exposure (Figure 3C; Table S4). Q111E and A112S each have significant effects individually (both  $\sim$ 2-fold), and their combined effects appear to be close to additive (Figure S3; Table S4). We also find that the substitutions Q111E and A112S cause slight neural dysfunction when introduced individually, and this dysfunction is exaggerated when they are combined (in ES flies; Figures 3D and S3). These results suggest that the substantial CTS resistance conferred by this combination is associated with negative pleiotropic effects on protein function. In *Photuris*, these may be compensated either by other substitutions in ATP $\alpha$ 1 paralogs B–D or by other mechanisms.

Although we did not generate lines representing the full complement of evolutionary paths along the paralogs B–D lineage, we find that substitution of T797I is homozygous lethal on the *D. melanogaster* ATP $\alpha$ 1 background. This is not unexpected given previous work showing that the similar substitution, T797V, decreases NKA activity to 3.4% of wild-type levels.<sup>38</sup>

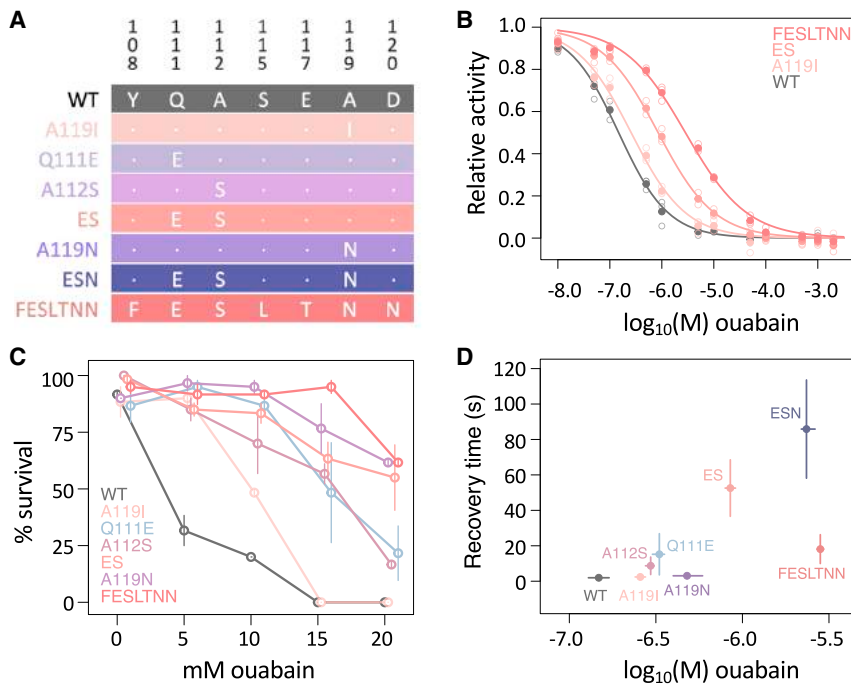


**Figure 3. Functional effects of *Photoris* paralogue-specific substitutions**

(A) Engineered fly lines generated in this study. Only sites implicated in CTS resistance are shown. States for the CTS-sensitive *D. melanogaster* strain (*w*<sup>1118</sup>) used to generate engineered lines are denoted “WT” for “wild type.” All strains were homozygous for the assayed substitutions. Detailed results for additional engineered lines can be found in [Figures S3 and S4](#).

(B) CTS-inhibition assays for NKA isolated from heads of WT and engineered fly lines. Mean relative activities (filled circles) are plotted as a function of increasing concentrations of ouabain, a representative CTS. Each mean is the average of three biological replicates. Solid lines represent the least squares fit model (as per [Figure 1](#); [STAR Methods](#); [Table S4](#)).

(C) CTS tolerance of WT and engineered adult flies. Survival of adult flies upon 7 days of exposure to increasing concentrations of ouabain. Points represent the average of three biological replicates (pools of *n* = 20 individuals), and whiskers correspond to standard errors. ESN could not be assayed here due to the poor condition of the line.

(D) Levels of neural dysfunction and enzyme resistance to ouabain for WT and engineered fly lines. The neural dysfunction assay (y axis) measures

the recovery time (seconds) following seizures induced by mechanical over-stimulation (aka the bang sensitivity assay) of adult male flies. 28–43 individuals are assayed for each line. The level of enzyme resistance to ouabain (x axis) is measured as IC50 in enzyme-inhibition assays (as per [Figure 1](#); [STAR Methods](#)). Plotted are the means and 95% bootstrap confidence bounds as points and whiskers, respectively.

Interestingly, the isoleucine at site 797 of *Photoris* ATP $\alpha$ 1B was replaced with valine after a second round of duplication (i.e., I797V; [Figure S1](#)). Additional engineering reveals that the combination Q111E + A112S + A119I + D120A (hereafter “ESIA”), occurring along the ATP $\alpha$ 1B lineage, is also homozygous lethal. It may be that the detrimental effects of ESIA and T797I (and subsequently I797V) observed on the *D. melanogaster* protein are ameliorated when combined (i.e., ESIAI/V) or by other substitutions in the ATP $\alpha$ 1 sequence background of fireflies. However, even if active and resistant, ATP $\alpha$ 1B has the lowest expression among the four paralogs ([Figure 2C](#)), implying that it may contribute little to overall CTS resistance in *Photoris*.

A more dramatic series of substitutions implicated in CTS resistance occurs along the lineage leading to *Photoris* ATP $\alpha$ 1 paralogs C and D ([Figure 2B](#)). We engineered most of these CTS-relevant substitutions (Y108F + Q111E + A112S + V115L + E117T + A119N + D120N, hereafter “FESLTNN”) into the *D. melanogaster* ATP $\alpha$ 1 protein. The FESLTNN combination results in an additional 3-fold increase in NKA CTS resistance over ES alone ([Figure 3B](#); [Table S4](#)). FESLTNN adults also exhibit exceptionally high rates of survival upon CTS exposure ([Figure 3C](#)). Further dissection of individual substitution effects reveals that A119N and the combination (Q111E + A112S + A119N, hereafter “ESN”) confer substantial CTS resistance to NKA (almost 3- and 16-fold, respectively). The level of NKA CTS resistance for ESN (16-fold) is only slightly lower than for FESLTNN (18-fold; [Table S4](#)), implying that the marginal effect of A119N is nearly sufficient to explain the difference between ES and FESLTNN. A119N alone also appears to be sufficient to confer levels of adult resistance to CTS exposure that are comparable to FESLTNN ([Figures 3 and S4C](#)).

Evaluation of the trade-offs associated with resistance conferred by various evolutionary intermediates offers further insight into the likely evolutionary paths used to evolve CTS resistance along the C/D paralogue lineage ([Figures 3D and S4](#)). Notably, ES confers substantial CTS resistance to the *D. melanogaster* protein, but at the cost of neurological defects ([Figure 3D](#)). Although adding A119N to the ES background (i.e., ESN) results in even higher CTS resistance, this comes at the cost of even greater neurological dysfunction. Interestingly, we find that ESN in combination with other substitutions added to the C/D paralogue lineage (i.e., FESLTNN) results in a similar level of CTS resistance but with substantially reduced neurological dysfunction. Taken together, our results reveal that serial rounds of gene duplication and neofunctionalization led to stepwise increases in the level of CTS resistance in *Photoris* over time, with substitutions A119I, Q111E + A112S, and I119N being key evolutionary steps. In addition, substitutions at other sites in *Photoris* NKAs, although not contributing much to resistance itself, nonetheless appear to play a critical role in ameliorating pleiotropic costs associated with key resistance substitutions. Similar patterns of background dependence (a.k.a. “intra-molecular epistasis”) have been observed in the evolution of CTS-resistant forms of NKA in insects and vertebrates,<sup>16,17,23,24,39</sup> the evolution of nicotinic acetylcholine receptor resistance to epibatidine in dendrobatid frogs,<sup>40</sup> and  $\gamma$ -aminobutyric acid (GABA) receptor resistance to the insecticide fipronil in plant hoppers.<sup>41</sup>

### The evolution of CTS resistance in prey firefly species

The *Photinus* NKA protein is also highly resistant to CTS inhibition *in vitro* ([Figure 1B](#)). However, in contrast to the dramatic patterns of neofunctionalization in *Photoris*, the sole copy of ATP $\alpha$ 1

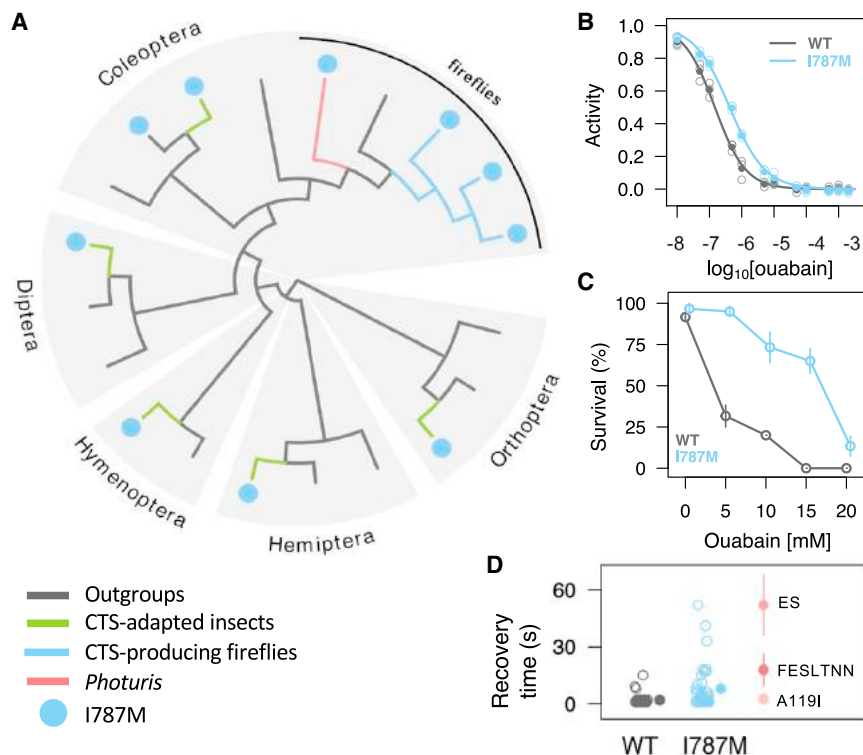


**Figure 4. Evolutionary and functional analysis reveals a new CTS-resistance substitution, I787M**

(A) Recurrent appearance of I787M in CTS-associated herbivores (green lineages), CTS-producing prey fireflies (blue lineages), and predatory *Photuris* fireflies (red lineage). See Figure S5 for more details.

(B) Estimates of the IC<sub>50</sub> of NKA of wild-type and engineered fly lines in CTS-inhibition assays. The log<sub>10</sub>(IC<sub>50</sub>) of I787M flies is 2.9-fold higher than that of WT (*w*<sup>1118</sup>) control flies (Table S4). Each estimate is based on three biological replicates (each with three technical replicates).

(C) CTS tolerance of adult wild-type and engineered flies. Engineered flies carrying I787M exhibit higher survival rates upon 7-day CTS exposure. Shown are means of three replicates with standard errors as whiskers.

(D) Neural dysfunction as measured by the bang sensitivity assay. The assay measures the time to recovery (seconds) from seizures induced by mechanical over-stimulation (as in Figure 3C). Open circles correspond to individual flies. Filled circles to the right are means with 95% CI. To the far right are means for ES, FESLTNN, and A119I with 95% CI whiskers, but individual data points are not shown. I787M individuals are somewhat more susceptible to mechanical over-stimulation than WT (Wilcoxon test  $p = 3.4e-5$ ), but the impairment is less severe than observed for some other engineered strains. See Figure 3D for more details on the A119I, ES, and FESLTNN lines.

in *Photinus* curiously lacks substitutions at known CTS-insensitivity sites other than V119I (Figures 2 and S1), which has a significant but relatively small effect (Figure 2B; Table S4). Notably absent in prey firefly species are substitutions at sites 111 and 122, which are most often associated with large effects on CTS resistance in species with a single copy of ATP $\alpha$ 1.<sup>21,22</sup>

In order to search for previously undocumented CTS-resistance sites throughout the protein, we queried all substitutions, naive to previously known functional importance, in a large alignment of ATP $\alpha$ 1 sequences from CTS-adapted and non-adapted insects (STAR Methods). Of the potential candidate substitutions in the *Photinus* lineage, only one (I787M) exhibits a strong signature of parallel evolution in multiple CTS-adapted taxa (Figures 4A and S5). Notably, I787M appears to be present in all CTS-producing firefly species surveyed here (*Lucidota*, *Ellychnia*, and *Photinus*) and is also present in paralogs C and D of *Photuris* (Figure S1). Using CRISPR-Cas9 engineering of *D. melanogaster*, we show that I787M has a significant effect on CTS resistance of the enzyme *in vitro* (a 3-fold increase; Figure 4B; Table S4). Despite its relatively modest effect on CTS resistance of the enzyme *in vitro*, I787M has a substantial effect on the tolerance of adult *D. melanogaster* to CTS exposure (Figure 4C) and is not associated with substantial neurological dysfunction (Figure 4D). Thus, I787M is a previously unreported determinant of CTS resistance that shows a high degree of parallelism among CTS-adapted insects.

## DISCUSSION

CTS resistance and the use of CTS for defense have convergently evolved in a large number of species. Our study reveals

that the first steps toward CTS-resistance evolution in fireflies (A119V, V119I) were likely taken before CTS synthesis evolved in *Photinus* and before predatory specialization on fireflies emerged in *Photuris*. One possible explanation for these shared steps is that *de novo* production of CTSs is ancestral to fireflies and that the ability to do this was subsequently lost in *Photuris* as they opted for predation as an alternative source of these toxins. However, there is little evidence for this based on the phylogenetic distribution of CTS production in fireflies<sup>1</sup> (Figure 4A). An alternative hypothesis is that these steps may reflect exaptations in fireflies unrelated to CTS metabolism. This is supported by the widespread distribution of substitutions at site 119 among insect taxa that are not adapted to CTSs,<sup>23</sup> including the Red Soldier Beetle surveyed here, which is closely related to fireflies. Interestingly, A119N—a key substitution underlying the resistance of neofunctionalized *Photuris* paralogs—is present in all Hymenopteran species surveyed to date.<sup>23</sup> As most Hymenopterans are not associated with CTSs, A119N may function as an exaptation that facilitated herbivorous wasp specialization on CTS-containing hostplants,<sup>42</sup> parasitoid wasp species predation on CTS-adapted herbivorous insects<sup>43</sup> or as generalist nectar feeders on the flowers of CTS-producing plants.<sup>44</sup>

Despite initial shared steps toward CTS resistance taken early in firefly diversification, our study also highlights the distinct dynamics of CTS-resistance evolution associated with their different ecological roles. Although both *Photuris* and other fireflies are protected by the same class of CTS toxins, they nonetheless face different biochemical and physiological challenges posed by *de novo* production (most firefly genera) versus sequestration from a food source (*Photuris*).<sup>30–32</sup> Notably, the dramatic repeated

duplication and neofunctionalization of ATP $\alpha$ 1 in *Photuris* resembles the strategy employed by several CTS-adapted herbivores that sequester CTSs from a food source.<sup>19,21,22,25</sup> We speculate that the duplication and neofunctionalization of ATP $\alpha$ 1 in *Photuris* may have been driven by the evolution of firefly predation in the *Photuris* lineage, which imposed similar biochemical and physiological challenges to those experienced by herbivores that sequester CTSs from hostplants.

We have shown that intermediate stages in the evolution of resistant forms of NKA in *Photuris* are associated with substantial enzymatic and physiological dysfunction when engineered into *D. melanogaster*. This dysfunction would likely represent a substantial negatively pleiotropic barrier to the evolution of CTS resistance if the ATP $\alpha$ 1 gene existed as a single copy in *Photuris*. The role of gene duplication as a solution to overcoming pleiotropic constraints associated with intermediate states has previously been proposed for genes involved in galactose metabolism in yeast,<sup>45</sup> ribonuclease genes in primates,<sup>46</sup> and the evolution of lens transparency in the eyes of vertebrates,<sup>47</sup> among other examples. We propose that these negative pleiotropic effects were largely avoided by duplication and neofunctionalization in the *Photuris* lineage, allowing this lineage to specialize on consuming and sequestering toxins from CTS-containing prey. Thus, our work implicates duplication and neofunctionalization as a potential factor in the diversification of species roles within an ecological community.

There is a strong association in insects between duplication and neofunctionalization of ATP $\alpha$ 1 and sequestering CTSs from a food source. Specifically, ATP $\alpha$ 1 in *Photuris* currently represents the 6<sup>th</sup> documented case with no counter-examples of duplications observed in non-sequestering species.<sup>21–23</sup> Despite this, there are several clear examples of species that sequester high levels of CTSs from a food source that lack neofunctionalized ATP $\alpha$ 1 duplications (e.g., the monarch butterfly). A related question is why CTS-producing firefly species lack duplication and neofunctionalization of ATP $\alpha$ 1 despite sequestering high levels of CTSs. The reasons for this difference may be manifold. First, although CTS-producing firefly species indeed store CTSs, they produce these compounds internally and do not absorb them from a food source. Additionally, even insect species that are not adapted to CTSs exhibit physiological features that at least partially protect them from the adverse effects of CTS exposure, including restricted expression of NKA to neurons (in Lepidoptera<sup>48</sup>) or expression of protective proteins that buffer the adverse effects of dietary CTSs (e.g., in Lepidoptera<sup>48</sup> and in *Drosophila*<sup>49</sup>). It is likely that the necessity of duplication and neofunctionalization of ATP $\alpha$ 1 depends on factors such as the amount of CTSs typically consumed, the polarity of these CTSs, and the permeability of tissues and cells to CTSs, among other factors. Further research is needed to determine which, if any, of these factors account for patterns of duplication and neofunctionalization of ATP $\alpha$ 1 in fireflies and other CTS-adapted insect species.

There remain some interesting and puzzling differences between insect herbivores and fireflies with respect to the molecular basis of CTS resistance via substitutions to ATP $\alpha$ 1. A recent study showed that three amino acid substitutions are sufficient to account for the entire difference in NKA CTS resistance observed between the wild-type proteins of *D. melanogaster* and the monarch butterfly, *Danaus plexippus*.<sup>24</sup> By contrast,

our attempts to engineer known CTS-resistance substitutions of fireflies into *D. melanogaster* NKA fall short of the level of CTS-resistance level of wild-type firefly proteins (Figure 5). This suggests wild-type firefly NKAs achieve high levels of CTS resistance via substitutions at other sites in ATP $\alpha$ 1. Previous attempts to map determinants of CTS resistance using saturation mutagenesis are likely to have missed sites with relatively small effects on CTS resistance.<sup>50</sup> This may explain why the I787M, discovered here using phylogenetic methods, was missed in previous screens for CTS-resistance mutations. The gap between engineered *Drosophila* and wild-type firefly NKA CTS resistance and the lack of obvious candidate substitutions in *Photinus* suggest that there are likely to be other, as yet undiscovered, determinants of CTS resistance in firefly NKAs.

#### DECLARATION OF GENERATIVE AI AND AI-ASSISTED TECHNOLOGIES IN THE WRITING PROCESS

During the preparation of this work, the author(s) used chatGPT in order to help improve the readability of some sections of this manuscript. After using this tool/service, the author(s) reviewed and edited the content as needed and take(s) full responsibility for the content of the publication.

#### STAR★METHODS

Detailed methods are provided in the online version of this paper and include the following:

- KEY RESOURCES TABLE
- RESOURCE AVAILABILITY
  - Lead Contact
  - Materials Availability
  - Data and Code Availability
- EXPERIMENTAL MODEL AND STUDY PARTICIPANT DETAILS
- METHOD DETAILS
  - Firefly collection and data sources
  - RNA-seq data generation and ATP $\alpha$ 1 reconstruction
  - Confirmation of ATP $\alpha$ 1 duplicates in *P. versicolor*
  - Phylogeny estimation and reconstruction of ancestral states
  - Differential expression analysis
  - CRISPR-cas9 engineered fly lines
  - Additional Lines Engineered Using the Method of Taverner et al.<sup>23</sup>
  - CTS tolerance assay
  - Enzyme inhibition assays
  - Bang-sensitivity assay
- QUANTIFICATION AND STATISTICAL ANALYSIS

#### SUPPLEMENTAL INFORMATION

Supplemental information can be found online at <https://doi.org/10.1016/j.cub.2023.10.063>.

#### ACKNOWLEDGMENTS

We thank the Fireflyers International Network for providing samples of *P. frontalis* (notably H. Morgan and P. Shaw) and their valuable natural history

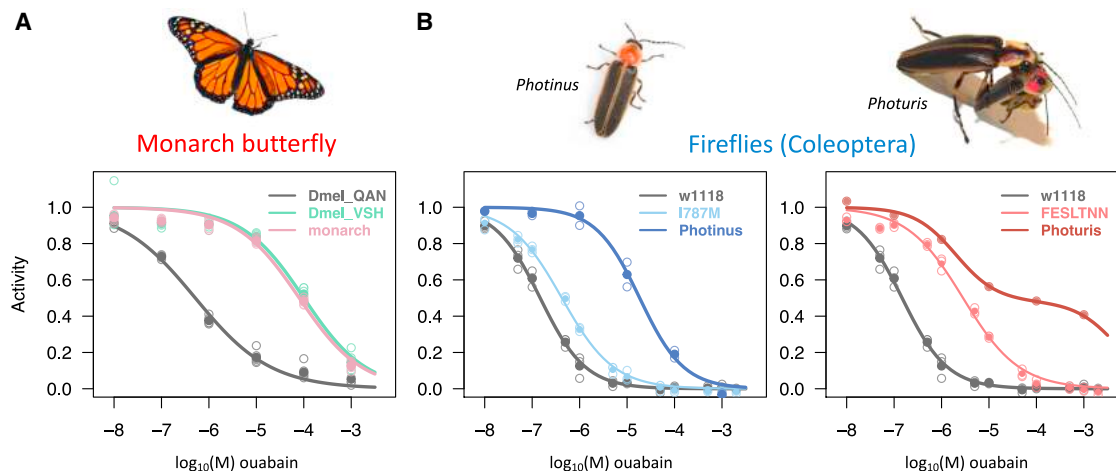


**Figure 5. CTS-inhibition curves suggest as yet unmapped determinants of CTS resistance in firefly  $\text{Na}^+, \text{K}^+$ -ATPases (NKAs)**

(A) Engineering three known CTS resistance-associated amino acid substitutions into *D. melanogaster* NKA accounts for ~100% of the CTS resistance of the monarch butterfly protein (data from Karageorgi et al.<sup>24</sup>). Plots are as in Figure 1. Dmel\_QAN, wild-type *D. melanogaster* protein; Dmel\_VSH, *D. melanogaster* protein + substitutions Q111V, A119S, and N122H; monarch, monarch butterfly (*Danaus plexippus*) protein. (B) By contrast, engineering the known major CTS-resistance substitutions observed in fireflies into *D. melanogaster* NKA results in only a fraction of the observed CTS resistance of the *Photinus* (left) and *Photuris* (right) proteins. The latter pattern points to as yet unmapped determinants of CTS resistance of firefly NKAs. w1118, wild-type *D. melanogaster*. The I787M and FESLTNN constructs are described in Figures 3 and 4, respectively. “*Photinus*” and “*Photuris*” are as in Figure 1.

input. We thank P. Reilly for advice on CRISPR-Cas9 design, A. Taverner for help with fly crosses, C. Han for advice on variant calling analysis, and M. Kardestuncer for help with collections. We thank S. Stiehler and M. Jang for technical assistance. Finally, we thank A.M. for inspiration. This work was funded by the National Institutes of Health R01 GM115523 to P.A., AG059385 to M.J.P., and DFG PE2059/3-1 and the LOEWE program of the State of Hesse (Insect Biotechnology & Bioresources), Germany, to G.P.

#### AUTHOR CONTRIBUTIONS

P.A. conceptualized the study. L.Y., F.B., M.L.A., R.V., M.W., and P.A. collected and prepared firefly samples. L.Y., F.B., Y.Z., M.L.A., and J.P. generated sequence data. L.Y., F.B., and P.A. performed data analysis. M.J.P., B.P.R., and A.D.T. generated phiC31/cre-lox engineered flies. L.Y. generated a subset of CRISPR-Cas9-engineered flies. L.Y., F.B., A.B., G.P., and P.A. designed and performed functional assays. Funding acquisition and supervision by P.A., M.J.P., and G.P. P.A. wrote the paper with input from the other authors.

#### DECLARATION OF INTERESTS

The authors declare no competing interests.

Received: May 23, 2023

Revised: September 4, 2023

Accepted: October 27, 2023

Published: November 20, 2023

#### REFERENCES

- Berger, A., Petschenka, G., Degenkolb, T., Geisthardt, M., and Vilcinskas, A. (2021). Insect collections as an untapped source of bioactive compounds—fireflies (Coleoptera: Lampyridae) and cardiotoxic steroids as a proof of concept. *Insects* 12, 689–698. <https://doi.org/10.3390/insects12080689>.
- Gronquist, M., Meinwald, J., Eisner, T., and Schroeder, F.C. (2005). Exploring uncharted terrain in nature's structure space using capillary NMR spectroscopy: 13 steroids from 50 fireflies. *J. Am. Chem. Soc.* 127, 10810–10811. <https://doi.org/10.1021/ja053617v>.
- Meinwald, J., Wiemer, D., and Eisner, T. (1979). Lucibufagins. 2. Esters of 12-oxo-2p,5p, 11 a-trihydroxybufalin, the major defensive steroids of the firefly *Photinus pyralis* (Coleoptera: Lampyridae). *J. Am. Chem. Soc.* 9, 3055–3060.
- Smedley, S.R., Risteen, R.G., Tonyai, K.K., Pitino, J.C., Hu, Y., Ahmed, Z.B., Christofel, B.T., Gaber, M., Howells, N.R., Mosey, C.F., et al. (2017). Bufadienolides (lucibufagins) from an ecologically aberrant firefly (*Ellychnia corrusca*). *Chemoecology* 27, 141–153. <https://doi.org/10.1007/s00049-017-0240-6>.
- Eisner, T., Wiemer, D.F., Haynes, L.W., and Meinwald, J. (1978). Lucibufagins: defensive steroids from the fireflies *Photinus ignitus* and *P. marginellus* (Coleoptera: Lampyridae). *Proc. Natl. Acad. Sci. USA* 75, 905–908. <https://doi.org/10.1073/pnas.75.2.905>.
- Tyler, J., McKinnon, W., Lord, G., and Hiltton, P. (2008). A defensive steroidal pyrone in the Glow-worm *Lampyrus noctiluca* L. (Coleoptera: Lampyridae). *Physiol. Entomol.* 33, 167–170.
- Lloyd, J.E. (1965). Aggressive mimicry in *Photuris*: firefly femmes fatales. *Science* 149, 653–654.
- Eisner, T., Goetz, M.A., Hill, D.E., Smedley, S.R., and Meinwald, J. (1997). Firefly “femmes fatales” acquire defensive steroids (lucibufagins) from their firefly prey. *Proc. Natl. Acad. Sci. USA* 94, 9723–9728.
- González, A., Hare, J.F., and Eisner, T. (1999). Chemical egg defense in *Photuris* firefly “femmes fatales”. *Chemoecology* 9, 177–185.
- Souto, P.M., Campello, L., Khattar, G., Miras Mermudes, J.R., Monteiro, R.F., and Lima da Silveira, L.F. (2019). How to design a predatory firefly? Lessons from the Photurinae (Coleoptera: Lampyridae). *Zool. Anz.* 278, 1–13. <https://doi.org/10.1016/j.jcz.2018.10.006>.
- Lewis, S.M., and Cratsley, C.K. (2008). Flash signal evolution, mate choice, and predation in fireflies. *Annu. Rev. Entomol.* 53, 293–321. <https://doi.org/10.1146/annurev.ento.53.103106.093346>.
- Blanco, G., and Mercer, R.W. (1998). Isozymes of the Na-K-ATPase: heterogeneity in structure, diversity in function. *Am. J. Physiol.* 44, F633–F650.
- Lingrel, J.B. (2010). The physiological significance of the cardiotoxic steroid/ouabain-binding site of the Na,K-ATPase. *Annu. Rev. Physiol.* 72, 395–412. <https://doi.org/10.1146/annurev-physiol-021909-135725>.

14. Dobler, S., Dalla, S., Wagschal, V., and Agrawal, A.A. (2012). Community-wide convergent evolution in insect adaptation to toxic cardenolides by substitutions in the Na,K-ATPase. *Proc. Natl. Acad. Sci. USA* *109*, 13040–13045. <https://doi.org/10.1073/pnas.1202111109>.
15. Holzinger, F., and Wink, M. (1996). Mediation of cardiac glycoside insensitivity in the monarch butterfly (*Danaus plexippus*): role of an amino acid substitution in the ouabain binding site of Na(+),K(+)-ATPase. *J. Chem. Ecol.* *22*, 1921–1937. <https://doi.org/10.1007/BF02028512>.
16. Mohammadi, S., Yang, L., Harpak, A., Herrera-Álvarez, S., del Pilar Rodríguez-Ordoñez, M., Peng, J., Zhang, K., Storz, J.F., Dobler, S., Crawford, A.J., et al. (2021). Concerted evolution reveals co-adapted amino acid substitutions in Na+K+-ATPase of frogs that prey on toxic toads. *Curr. Biol.* *31*, 2530–2538.e10. <https://doi.org/10.1016/j.cub.2021.03.089>.
17. Mohammadi, S., Herrera-Álvarez, S., Yang, L., Rodríguez-Ordoñez, M.D.P., Zhang, K., Storz, J.F., Dobler, S., Crawford, A.J., and Andolfatto, P. (2022). Constraints on the evolution of toxin-resistant Na,K-ATPases have limited dependence on sequence divergence. *PLoS Genet.* *18*, e1010323. <https://doi.org/10.1371/journal.pgen.1010323>.
18. Moore, D.J., Halliday, D.C.T., Rowell, D.M., Robinson, A.J., and Keogh, J.S. (2009). Positive Darwinian selection results in resistance to cardioactive toxins in true toads (*Anura*: Bufonidae). *Biol. Lett.* *5*, 513–516. <https://doi.org/10.1098/rsbl.2009.0281>.
19. Petschenka, G., Wagschal, V., Von Tschirnhaus, M., Donath, A., Dobler, S., and Koenig, F.A. (2017). Convergently evolved toxic secondary metabolites in plants drive the parallel molecular evolution of insect resistance. *Am. Nat.* *190*, S29–S43. <https://doi.org/10.5061/dryad.20191>.
20. Ujvari, B., Casewell, N.R., Sunagar, K., Arbuckle, K., Wüster, W., Lo, N., O’Meally, D., Beckmann, C., King, G.F., Deplazes, E., et al. (2015). Widespread convergence in toxin resistance by predictable molecular evolution. *Proc. Natl. Acad. Sci. USA* *112*, 11911–11916. <https://doi.org/10.1073/pnas.1511706112>.
21. Yang, L., Ravikanthachari, N., Mariño-Pérez, R., Deshmukh, R., Wu, M., Rosenstein, A., Kunte, K., Song, H., and Andolfatto, P. (2019). Predictability in the evolution of Orthopteran cardenolide insensitivity. *Philos. Trans. R. Soc. Lond. B Biol. Sci.* *374*, 20180246. <https://doi.org/10.1098/rstb.2018.0246>.
22. Zhen, Y., Aardema, M.L., Medina, E.M., Schumer, M., and Andolfatto, P. (2012). Parallel molecular evolution in an herbivore community. *Science* *337*, 1634–1637.
23. Taverner, A.M., Yang, L., Barile, Z.J., Lin, B., Peng, J., Pinharanda, A.P., Rao, A.S., Roland, B.P., Talsma, A.D., Wei, D., et al. (2019). Adaptive substitutions underlying cardiac glycoside insensitivity in insects exhibit epistasis in vivo. *eLife* *8*, e48224. <https://doi.org/10.7554/eLife.48224>.
24. Karageorgi, M., Groen, S.C., Sumbul, F., Pelaez, J.N., Verster, K.I., Aguilar, J.M., Hastings, A.P., Bernstein, S.L., Matsunaga, T., Astourian, M., et al. (2019). Genome editing retraces the evolution of toxin resistance in the monarch butterfly. *Nature* *574*, 409–412. <https://doi.org/10.1038/s41586-019-1610-8>.
25. Dobler, S., Wagschal, V., Pietsch, N., Dahdoui, N., Meinzer, F., Romey-GlÜsing, R., and Schütte, K. (2019). New ways to acquire resistance: imperfect convergence in insect adaptations to a potent plant toxin. *Proc. Biol. Sci.* *286*, 20190883. <https://doi.org/10.1098/rspb.2019.0883>.
26. Fallon, T.R., Lower, S.E., Chang, C.H., Bessho-Uehara, M., Martin, G.J., Bewick, A.J., Behringer, M., Debat, H.J., Wong, I., Day, J.C., et al. (2018). Firefly genomes illuminate parallel origins of bioluminescence in beetles. *eLife* *7*, e36495. <https://doi.org/10.7554/eLife.36495>.
27. Oba, Y., Konishi, K., Yano, D., Shibata, H., Kato, D., and Shirai, T. (2020). Resurrecting the ancient glow of the fireflies. *Sci. Adv.* *6*, eabc5705. <https://doi.org/10.1126/sciadv.abc5705>.
28. Branham, M.A., and Wenzel, J.W. (2003). The origin of photic behavior and the evolution of sexual communication in fireflies (Coleoptera: Lampyridae). *Cladistics* *19*, 1–22. <https://doi.org/10.1111/j.1096-0031.2003.tb00404.x>.
29. Lloyd, J.E. (1973). Firefly parasites and predators. *Coleopt. Bull.* *27*, 91–106.
30. González, A., Schroeder, F.C., Attygalle, A.B., Svatos, A., Meinwald, J., and Eisner, T. (1999). Metabolic transformations of acquired lucibufagins by firefly “femmes fatales”. *Chemoecology* *9*, 105–112.
31. Heckel, D.G. (2014). Insect detoxification and sequestration strategies. In *Annual Plant Reviews*, C. Voelckel, and G. Jander, eds. (John Wiley & Sons, Ltd), pp. 77–114. <https://doi.org/10.1002/9781118829783.ch3>.
32. Petschenka, G., and Agrawal, A.A. (2016). How herbivores coopt plant defenses: natural selection, specialization, and sequestration. *Curr. Opin. Insect Sci.* *14*, 17–24. <https://doi.org/10.1016/j.cois.2015.12.004>.
33. Höhna, S., Lower, S.E., Duchon, P., and Catalán, A. (2022). A time-calibrated firefly (Coleoptera: Lampyridae) phylogeny: using genomic data for divergence time estimation. Preprint at bioRxiv. <https://doi.org/10.1101/2021.11.19.469195v2>.
34. Martin, G.J., Branham, M.A., Whiting, M.F., and Bybee, S.M. (2017). Total evidence phylogeny and the evolution of adult bioluminescence in fireflies (Coleoptera: Lampyridae). *Mol. Phylogenet. Evol.* *107*, 564–575. <https://doi.org/10.1016/j.ympev.2016.12.017>.
35. Chen, X., Dong, Z., Liu, G., He, J., Zhao, R., Wang, W., Peng, Y., and Li, X. (2019). Phylogenetic analysis provides insights into the evolution of Asian fireflies and adult bioluminescence. *Mol. Phylogenet. Evol.* *140*, 106600. <https://doi.org/10.1016/j.ympev.2019.106600>.
36. Ganetzky, B., and Wu, C.F. (1982). Indirect suppression involving behavioral mutants with altered nerve excitability in *Drosophila melanogaster*. *Genetics* *100*, 597–614. <https://doi.org/10.1093/GENETICS/100.4.597>.
37. Laursen, M., Gregersen, J.L., Yatime, L., Nissen, P., and Fedosova, N.U. (2015). Structures and characterization of digoxin- and bufalin-bound Na+,K+-ATPase compared with the ouabain-bound complex. *Proc. Natl. Acad. Sci. USA* *112*, 1755–1760. <https://doi.org/10.1073/PNAS.1422997112>.
38. Feng, J., and Lingrel, J.B. (1994). Analysis of amino acid residues in the H5-H6 transmembrane and extracellular domains of Na,K-ATPase alpha subunit identifies threonine 797 as a determinant of ouabain sensitivity. *Biochemistry* *33*, 4218–4224.
39. Mohammadi, S., Özdemir, H.İ., Ozbek, P., Sumbul, F., Stiller, J., Deng, Y., Crawford, A.J., Rowland, H.M., Storz, J.F., Andolfatto, P., et al. (2022). Epistatic effects between amino acid insertions and substitutions mediate toxin resistance of vertebrate Na+,K+-ATPases. *Mol. Biol. Evol.* *39*, msac258. <https://doi.org/10.1093/molbev/msac258>.
40. Tarvin, R.D., Borghese, C.M., Sachs, W., Santos, J.C., Lu, Y., O’Connell, L.A., Cannatella, D.C., Harris, R.A., and Zakon, H.H. (2017). Interacting amino acid replacements allow poison frogs to evolve epibatidine resistance. *Science* *357*, 1261–1266. <https://doi.org/10.1126/science.aan5061>.
41. Zhang, Y., Meng, X., Yang, Y., Li, H., Wang, X., Yang, B., Zhang, J., Li, C., Millar, N.S., and Liu, Z. (2016). Synergistic and compensatory effects of two point mutations conferring target-site resistance to fipronil in the insect GABA receptor RDL. *Sci. Rep.* *6*, 32335. <https://doi.org/10.1038/srep32335>.
42. Dobler, S., Petschenka, G., Wagschal, V., and Flacht, L. (2015). Convergent adaptive evolution - how insects master the challenge of cardiac glycoside-containing host plants. *Entomol. Exp. Appl.* *157*, 30–39. <https://doi.org/10.1111/eea.12340>.
43. Groen, S.C., and Whiteman, N.K. (2021). Convergent evolution of cardiac glycoside resistance in predators and parasites of milkweed herbivores. *Curr. Biol.* *31*, R1465–R1466. <https://doi.org/10.1016/j.CUB.2021.10.025>.
44. Manson, J.S., Rasmann, S., Halitschke, R., Thomson, J.D., and Agrawal, A.A. (2012). Cardenolides in nectar may be more than a consequence of allocation to other plant parts: a phylogenetic study of *Asclepias*. *Funct. Ecol.* *26*, 1100–1110. <https://doi.org/10.1111/j.1365-2435.2012.02039.x>.
45. Hittinger, C.T., and Carroll, S.B. (2007). Gene duplication and the adaptive evolution of a classic genetic switch. *Nature* *449*, 677–681. <https://doi.org/10.1038/nature06151>.
46. Zhang, J., Rosenberg, H.F., and Nei, M. (1998). Positive Darwinian selection after gene duplication in primate ribonuclease genes. *Proc. Natl. Acad. Sci. USA* *95*, 3708–3713. <https://doi.org/10.1073/pnas.95.7.3708>.

47. Piatigorsky, J., O'Brien, W.E., Norman, B.L., Kalumuck, K., Wistow, G.J., Borras, T., Nickerson, J.M., and Wawrousek, E.F. (1988). Gene sharing by delta-crystallin and argininosuccinate lyase. *Proc. Natl. Acad. Sci. USA* *85*, 3479–3483. <https://doi.org/10.1073/pnas.85.10.3479>.
48. Petschenka, G., Pick, C., Wagschal, V., and Dobler, S. (2013). Functional evidence for physiological mechanisms to circumvent neurotoxicity of cardenolides in an adapted and a non-adapted hawk-moth species. *Proc. Biol. Sci.* *280*, 20123089. <https://doi.org/10.1098/rspb.2012.3089>.
49. Groen, S.C., LaPlante, E.R., Alexandre, N.M., Agrawal, A.A., Dobler, S., and Whiteman, N.K. (2017). Multidrug transporters and organic anion transporting polypeptides protect insects against the toxic effects of cardenolides. *Insect Biochem. Mol. Biol.* *81*, 51–61. <https://doi.org/10.1016/j.ibmb.2016.12.008>.
50. Croyle, M.L., Woo, A.L., and Lingrel, J.B. (1997). Extensive random mutagenesis analysis of the Na<sup>+</sup>/K<sup>+</sup>-ATPase alpha subunit identifies known and previously unidentified amino acid residues that alter ouabain sensitivity Implications for ouabain binding. *Eur. J. Biochem.* *248*, 488–495.
51. Martin, M. (2011). Cutadapt removes adapter sequences from high-throughput sequencing reads. *EMBnet J.* *17*, 10. <https://doi.org/10.14806/ej.17.1.200>.
52. Haas, B.J., Papanicolaou, A., Yassour, M., Grabherr, M., Blood, P.D., Bowden, J., Couger, M.B., Eccles, D., Li, B., Lieber, M., et al. (2013). De novo transcript sequence reconstruction from RNA-seq using the Trinity platform for reference generation and analysis. *Nat. Protoc.* *8*, 1494–1512. <https://doi.org/10.1038/nprot.2013.084>.
53. Zerbino, D.R., and Birney, E. (2008). Velvet: algorithms for de novo short read assembly using de Bruijn graphs. *Genome Res.* *18*, 821–829. <https://doi.org/10.1101/gr.074492.107>.
54. Schulz, M.H., Zerbino, D.R., Vingron, M., and Birney, E. (2012). Oases: robust de novo RNA-seq assembly across the dynamic range of expression levels. *Bioinformatics* *28*, 1086–1092. <https://doi.org/10.1093/bioinformatics/bts094>.
55. Gouy, M., Guindon, S., and Gascuel, O. (2010). SeaView version 4: a multi-platform graphical user interface for sequence alignment and phylogenetic tree building. *Mol. Biol. Evol.* *27*, 221–224. <https://doi.org/10.1093/molbev/msp259>.
56. Li, H., Handsaker, B., Wysoker, A., Fennell, T., Ruan, J., Homer, N., Marth, G., Abecasis, G., and Durbin, R.; 1000 Genome Project Data Processing Subgroup (2009). The Sequence Alignment/Map format and SAMtools. *Bioinformatics* *25*, 2078–2079. <https://doi.org/10.1093/bioinformatics/btp352>.
57. Yang, Z. (2007). PAML 4: phylogenetic analysis by maximum likelihood. *Mol. Biol. Evol.* *24*, 1586–1591. <https://doi.org/10.1093/molbev/msm088>.
58. Putri, G.H., Anders, S., Pyl, P.T., Pimanda, J.E., and Zanini, F. (2022). Analysing high-throughput sequencing data in Python with HTSeq 2.0. *Bioinformatics* *38*, 2943–2945. <https://doi.org/10.1093/bioinformatics/btac166>.
59. Love, M.I., Huber, W., and Anders, S. (2014). Moderated estimation of fold change and dispersion for RNA-seq data with DESeq2. *Genome Biol.* *15*, 550. <https://doi.org/10.1186/s13059-014-0550-8>.
60. Li, H. (2013). Aligning sequence reads, clone sequences and assembly contigs with BWA-MEM. Preprint at arXiv. <https://doi.org/10.48550/arXiv.1303.3997>.
61. Picelli, S., Björklund, A.K., Reinius, B., Sagasser, S., Winberg, G., and Sandberg, R. (2014). Tn5 transposase and tagmentation procedures for massively scaled sequencing projects. *Genome Res.* *24*, 2033–2040. <https://doi.org/10.1101/gr.177881.114>.
62. Pham, T.V., and Jimenez, C.R. (2012). An accurate paired sample test for count data. *Bioinformatics* *28*, i596–i602. <https://doi.org/10.1093/bioinformatics/bts394>.
63. Kondo, S., and Ueda, R. (2013). Highly improved gene targeting by germline-specific Cas9 expression in *Drosophila*. *Genetics* *195*, 715–721. <https://doi.org/10.1534/genetics.113.156737>.
64. Richardson, C.D., Ray, G.J., DeWitt, M.A., Curie, G.L., and Com, J.E. (2016). Enhancing homology-directed genome editing by catalytically active and inactive CRISPR-Cas9 using asymmetric donor DNA. *Nat. Biotechnol.* *34*, 339–344. <https://doi.org/10.1038/nbt.3481>.
65. Palladino, M.J., Bower, J.E., Kreber, R., and Ganetzky, B. (2003). Neural dysfunction and neurodegeneration in *Drosophila* Na<sup>+</sup>/K<sup>+</sup> ATPase alpha subunit mutants. *J. Neurosci.* *23*, 1276–1286. <https://doi.org/10.1523/JNEUROSCI.23-04-01276.2003>.

STAR★METHODS

KEY RESOURCES TABLE

REAGENT or RESOURCE	SOURCE	IDENTIFIER
<b>Chemicals, peptides, and recombinant proteins</b>		
RNAlater	Invitrogen	AM7020
TRIzol	Ambion, Life Technologies	15596018
Phusion High-Fidelity DNA Polymerase	Thermo Fisher Scientific	F530
Taq polymerase	New England Biolabs	M0273
Ouabain octahydrate	Sigma-Aldrich	Cat# O-3125
Nutri-fly Instant media	Flystuff	66-117
<b>Critical commercial assays</b>		
TruSeq RNA Library Prep Kit v2	Illumina	RS-122-2001
TruSeq Stranded mRNA	Illumina	20020594
QIAquick PCR Purification Kit	Qiagen	28104
MEGAscript T7 Transcription Kit	Invitrogen	AMB13345
Quick-change Lightning site-directed mutagenesis kit	Agilent	210518
<b>Deposited data</b>		
RNAseq data for firefly tissues	This study	SRA: PRJNA891306, PRJNA922528, PRJNA891248
ATP $\alpha$ 1 coding sequences	This study	GenBank: MT897473.1 to MT897482.1
<b>Experimental models: Organisms/strains</b>		
<i>Drosophila melanogaster</i> injection strain	Well Genetics	w1118
<i>Drosophila melanogaster</i> injection strain with germline Cas9 expression	Well Genetics	w1118; attP40{nos-Cas9} / CyO
<i>Drosophila melanogaster</i> w[*];; TM6B, Tb[1] / TM2, y+	Well Genetics	w[*];;TM6B, Tb[1] / TM2, y+
<i>Drosophila melanogaster</i> w[*]; CyO, P{Tub-PBac}/ Sp; +/TM6B	Bloomington Drosophila Stock Center	Bloomington #8285
<i>Drosophila melanogaster</i> w[*]; TM3, Sb[1] Ser[1]/TM6B, Tb[1]	Bloomington Drosophila Stock Center	Bloomington #2537
<i>Drosophila melanogaster</i> y1, w67c23, P{y[+mDint2]=Crey}1b;; D*/TM3, Sb1	Bloomington Drosophila Stock Center	Bloomington #851
<i>Drosophila melanogaster</i> w*;;ry506 Dr1/TM6B, P{w[+mC]=Dfd-EYFP}3, Sb1,Tb1,ca1	Bloomington Drosophila Stock Center	Bloomington #8704
<i>Drosophila melanogaster</i> A119I	This study	A119I
<i>Drosophila melanogaster</i> Y108F-Q111E-A112S-S115L-E117T-A119N-D120N	This study	FESLTNN
<i>Drosophila melanogaster</i> Q111E-A112S-A119I-D120A/TM6,Tb	This study	ESIA/TM6,Tb
<i>Drosophila melanogaster</i> T797I/TM6,EYFP	This study	T797I/TM6,EYFP
<i>Drosophila melanogaster</i> F786Y	This study	F786Y
<i>Drosophila melanogaster</i> I787M	This study	I787M
<i>Drosophila melanogaster</i> founder strain for targeted editing	Taverner et al. <sup>23</sup>	w1118;;ATP $\alpha$ Δ2-6b attP/TM6B,Tb1
<i>Drosophila melanogaster</i> Q111E	This study	Q111E
<i>Drosophila melanogaster</i> A112S	This study	A112S

(Continued on next page)

**Continued**

REAGENT or RESOURCE	SOURCE	IDENTIFIER
<i>Drosophila melanogaster</i> A119N	This study	A119N
<i>Drosophila melanogaster</i> Q111E+A112S	This study	ES
<i>Drosophila melanogaster</i> Q111E+A112S+A119N	This study	ESN
<b>Oligonucleotides</b>		
Forward PCR primer <i>Photuris versicolor</i> ATP $\alpha$ paralog A	This study	Ptu_ver_AF: CGCTGACTTTGATTCATCCCCAGT
Reverse PCR primer <i>Photuris versicolor</i> ATP $\alpha$ paralog A	This study	Ptu_ver_AR: TTGGCAGTGCGCATCATTCT
Forward PCR primer <i>Photuris versicolor</i> ATP $\alpha$ paralog B	This study	Ptu_ver_BF: TCGGAGTTTGGCCGTACAGA
Reverse PCR primer <i>Photuris versicolor</i> ATP $\alpha$ paralog B	This study	Ptu_ver_BR: TTGGTCAGTGAACGGCAGTG
Forward PCR primer <i>Photuris versicolor</i> ATP $\alpha$ paralog C	This study	Ptu_ver_CF: TCGACTTCAGGATTTGTTGACGG
Reverse PCR primer <i>Photuris versicolor</i> ATP $\alpha$ paralog C	This study	Ptu_ver_CR: TGGCAGTACGCACCATTAC
Forward PCR primer <i>Photuris versicolor</i> ATP $\alpha$ paralog D	This study	Ptu_ver_DF: CGTTCAGACTCATACCGTGTAGC
Reverse PCR primer <i>Photuris versicolor</i> ATP $\alpha$ paralog D	This study	Ptu_ver_DR: TGAACTCATCCGTAACCATGCAG
CRISPR reagents	This study	See <a href="#">Table S3</a>
<b>Recombinant DNA</b>		
TOPO TA-cloning vector	Invitrogen	K457502
Expression vector containing a U6 promoter	Well genetics	pBFv-U6.2
Expression vector for germline Cas9 expression	Well genetics	pBFv-nosP-Cas9
Plasmid donor template for A119I	This study	pUC57-Kan-A119I-pBacDsRed
Plasmid donor template for “ESIA”	This study	pUC57-Kan-Q111E-A112S-A119I-D120A-pBacDsRed
Plasmid donor template for “FESSLTN”	This study	pUC57-Kan-Y108F-Q111E-A112S-S115L-E117T-A119N-D120N-pBacDsRed
Plasmid donor template for T797I	This study	pUC57-Kan-T797I-pBacDsRed
Vector for targeted editing of exons 2-6 of ATP $\alpha$	Taverner et al. <sup>23</sup>	pGX-attB-ATP $\alpha$ $\Delta$ 2-6b
<b>Software and algorithms</b>		
TQSfastq.py	Howard Hughes Medical Institute	<a href="https://github.com/JaneliaSciComp/msg/blob/master/TQSfastq.py">https://github.com/JaneliaSciComp/msg/blob/master/TQSfastq.py</a>
trim_galore	N/A	<a href="https://github.com/FelixKrueger/TrimGalore">https://github.com/FelixKrueger/TrimGalore</a>
cutadapt	Martin <sup>51</sup>	<a href="https://cutadapt.readthedocs.io/">https://cutadapt.readthedocs.io/</a>
Trinity	Haas et al. <sup>52</sup>	<a href="https://github.com/trinityrnaseq/trinityrnaseq/wiki">https://github.com/trinityrnaseq/trinityrnaseq/wiki</a>
Picard	Broad Institute	<a href="https://broadinstitute.github.io/picard/">https://broadinstitute.github.io/picard/</a>
Velvet	Zerbino and Birney <sup>53</sup>	<a href="https://github.com/dzerbino/velvethttps://github.com/dzerbino/velvet">https://github.com/dzerbino/velvethttps://github.com/dzerbino/velvet</a>
Oases	Schulz et al. <sup>54</sup>	<a href="https://github.com/dzerbino/oases">https://github.com/dzerbino/oases</a>
SeaView	Gouy et al. <sup>55</sup>	<a href="https://doua.prabi.fr/software/seaview">https://doua.prabi.fr/software/seaview</a>
Samtools	Li et al. <sup>56</sup>	<a href="https://github.com/samtools/samtools">https://github.com/samtools/samtools</a>
BLAST	NCBI	<a href="https://blast.ncbi.nlm.nih.gov/Blast.cgi">https://blast.ncbi.nlm.nih.gov/Blast.cgi</a>
MUSCLE	EMBL-EBI	<a href="https://www.ebi.ac.uk/Tools/msa/muscle/">https://www.ebi.ac.uk/Tools/msa/muscle/</a>
Gatk3	Broad Institute	<a href="https://gatk.broadinstitute.org/hc/en-us">https://gatk.broadinstitute.org/hc/en-us</a>
Geneious prime	Domatics	<a href="https://www.geneious.com/">https://www.geneious.com/</a>
PhyML	ATGC Montpellier	<a href="http://www.atgc-montpellier.fr/phyml/">http://www.atgc-montpellier.fr/phyml/</a>
PAML	Yang <sup>57</sup>	<a href="http://abacus.gene.ucl.ac.uk/software/paml.html">http://abacus.gene.ucl.ac.uk/software/paml.html</a>
gmod_fasta2gff3.pl	N/A	<a href="https://github.com/GMOD/Chado/">https://github.com/GMOD/Chado/</a>
htseq-count	Putri et al. <sup>58</sup>	<a href="https://htseq.readthedocs.io/en/master/index.html">https://htseq.readthedocs.io/en/master/index.html</a>
Deseq2 R package	Love et al. <sup>59</sup>	<a href="https://bioconductor.org/packages/release/bioc/html/DESeq2.html">https://bioconductor.org/packages/release/bioc/html/DESeq2.html</a>
Minipack.lm R package	N/A	<a href="https://cran.r-project.org/web/packages/minipack.lm/index.html">https://cran.r-project.org/web/packages/minipack.lm/index.html</a>

(Continued on next page)

**Continued**

REAGENT or RESOURCE	SOURCE	IDENTIFIER
Variant calling scripts	N/A	<a href="https://github.com/YourePrettyGood/PseudoreferencePipeline">https://github.com/YourePrettyGood/PseudoreferencePipeline</a>
bwa mem	Li <sup>60</sup>	<a href="https://janis.readthedocs.io/en/latest/tools/bioinformatics/bwa/bwamem.html">https://janis.readthedocs.io/en/latest/tools/bioinformatics/bwa/bwamem.html</a>

**RESOURCE AVAILABILITY**

**Lead Contact**

Further information and requests on methods can be directed to Dr. Peter Andolfatto [pa2543@columbia.edu](mailto:pa2543@columbia.edu)

**Materials Availability**

Plasmids used in this study are available upon request. This study did not generate new unique reagents.

**Data and Code Availability**

Data generated during this study are available through links provided in the [key resources table](#). Nucleotide sequences (CDS) of ATP $\alpha$ 1 have been submitted to GenBank (GenBank: MT897473-MT897482). RNA-seq data for *Photinus pyralis* and *Photuris versicolor* have been deposited in the Sequence Read Archive (BioProject PRJNA891248, PRJNA891306, PRJNA922528). This paper does not report original code. Any additional information required to reanalyze the data reported in this work paper is available from the [lead contact](#) upon request.

**EXPERIMENTAL MODEL AND STUDY PARTICIPANT DETAILS**

Wild specimens of adult *Photinus pyralis* and *Photuris versicolor* were used. The origin of all *Drosophila* fly strains used can be found in the [key resources table](#). All flies were cultured on standard cornmeal-agar medium in uncrowded conditions unless stated in the methods.

**METHOD DETAILS**

**Firefly collection and data sources**

*Photuris versicolor* and *Photinus pyralis* were collected in Princeton, NJ, USA during the summer months of 2017, 2018 and 2022. Specimens of *Rhagonycha fulva* were collected in Stuttgart, Germany in July 2023. Samples were immediately stored at -80°C with or without RNAlater (Invitrogen™) depending on the planned downstream experiments. For other species, we used publicly available data (see [Table S1](#)).

**RNA-seq data generation and ATP $\alpha$ 1 reconstruction**

Total RNA from muscle (thoracic or leg), heads and gut of male *Photinus*, female and male *Photuris* fireflies was extracted with TRIzol (Ambion, Life Technologies) following the manufacturer's protocol. For male *Photinus* and female *Photuris* samples, RNA-seq libraries were prepared with TruSeq RNA Library Prep Kit v2 (Illumina) and sequenced on a HiSeq4000 (Genewiz, South Plainfield, NJ, USA). Reads were trimmed for quality and length using TQSFastq.py ([key resources table](#)) with default parameters. For male *Photuris* samples, RNA-seq libraries were prepared with TruSeq Stranded mRNA Library Prep (Illumina) and sequenced on HiSeq X (PSOMAGEN, Inc.). Reads were trimmed for adapters but not for quality using trim\_galore (v0.6.7) with cutadapt (v1.18). The three RNA-seq datasets were used to generate *de novo* transcriptome assemblies using Trinity v2.2.0<sup>52</sup> with default parameters. Beetle ATP $\alpha$ 1 sequences<sup>22</sup> were used as initial queries to BLAST (BLAST 2.13.0+ with default parameters) against firefly transcriptome assemblies. Reconstructed ATP $\alpha$ 1 sequences for *Photinus pyralis* and *Photuris versicolor* were then used as templates to identify ATP $\alpha$ 1 sequences in *de novo* transcriptome and genome assemblies from other firefly species.

Since *de novo* assembly of *P. versicolor* revealed four distinct paralogs of ATP $\alpha$ 1, we set out to determine the ages of duplication events by surveying closely related species *Photuris frontalis* and *Bicellonycha wickershamorum* ([Table S1](#)). We searched for ATP $\alpha$ 1 homologs in the *de novo* transcriptomes of *P. frontalis* and *B. wickershamorum* using BLAST (tblastn, BLAST 2.13.0+,  $value=1e-50$ ). Orthologs of all four *P. versicolor* paralogs we unambiguously identified in *P. frontalis*. To reconstruct the *P. frontalis* paralogs, RNA-seq reads were mapped to *P. versicolor* paralogs using bwa mem (v 0.7.17) as described above. Duplicates were identified and reads were assigned a read-group using Picard (v 2.27.5). BAM files were sorted and indexed using Samtools (v 1.6). Reads were then realigned using GATK3 (v 3.8.1) and variants were called using the YourePrettyGood pseudoreference pipeline ([key resources table](#); samtoolsVariantCall.sh and vcfToPseudoref.sh with thresholds MQ  $\leq 20$ , QUAL  $\leq 26$ ). bcftools (v1.9) was then used to create an inferred sequence for each paralog.

In contrast to *P. frontalis*, we detected only one copy of ATP $\alpha$ 1 in the *B. wickershamorum de novo* transcriptome. The top BLAST hit shares 97.7% amino acid identity with the *P. versicolor* paralog A (score= 1882, evalue=0.0). The second-best hit (score=326, evalue=3e-94) shares only ~25% amino acid identity with *P. versicolor* ATP $\alpha$ 1 paralogs. The latter protein is most likely to be sarco/endoplasmic reticulum-type Ca<sup>2+</sup>-ATPase based on comparisons to the *D. melanogaster* genome annotation (with which it has 80% amino acid sequence identity). In a second attempt to detect possible duplications in *B. wickershamorum*, we mapped RNAseq reads to its ATP $\alpha$ 1 and looked for potential amino acid variants supported by three or more reads. Only one amino acid variant was found at position 830 (D/E), but this site has not been implicated in CTS resistance. These lines of evidence suggest that *B. wickershamorum* lacks neofunctionalized duplications ATP $\alpha$ 1, or that they are not expressed.

### Confirmation of ATP $\alpha$ 1 duplicates in *P. versicolor*

The four reconstructed ATP $\alpha$ 1 paralogs (A–D) of *Photuris versicolor* were confirmed by PCR-cloning and sequencing (see [key resources table](#) for primers used). ATP $\alpha$ 1 paralogs were amplified from cDNA using Phusion High-Fidelity DNA Polymerase (Thermo Fisher Scientific) and separated by agarose gel electrophoresis. The appropriate bands were gel-extracted and cleaned with QIAquick PCR Purification Kit (Qiagen). Purified PCR products were 3'A-tailed using Taq polymerase (NEB) and cloned into TOPO TA-cloning vector (Invitrogen). Plasmids with inserts were identified and isolated using colony-PCR. Tn5-tagmentation libraries<sup>61</sup> were prepared for each plasmid and indexed using customized Illumina-style i7 and i5 PCR primers added with 10 cycles of PCR. The libraries were pooled and sequenced with 150 nt, paired-end reads on an Illumina MiSeq Nano flowcell. 10,000 pair-end reads per plasmid were randomly sampled, trimmed for quality and *de novo* assembled using Velvet<sup>53</sup> and Oases.<sup>54</sup> The sequences for each paralog were aligned and visualized in SeaView.<sup>55</sup>

### Phylogeny estimation and reconstruction of ancestral states

Firefly ATP $\alpha$ 1 protein-coding sequences together with ATP $\alpha$ 1 sequences of *D. melanogaster*, *Agrilus planipennis* and the soldier beetles *Chauliognathus marginatus* and *Rhagonycha fulva* ([Table S1](#)) were aligned using MUSCLE (v 3.8.425). The sequences were trimmed to produce an alignment with no gaps or missing data. A phylogenetic tree for ATP $\alpha$ 1 sequences was estimated using maximum likelihood with PhyML (v 3.3.20180621) with the GTR model and default parameters. Ancestral sequences and substitutions along specific-lineages were estimated based on this alignment and the tree using PAML's baseml function (v 4.9) with the following parameters: model=7, kappa=1.6, RateAncestor=2.<sup>57</sup>

To look for substitutions that occur recurrently in CTS-associated species, we combined the multispecies alignment of Taverner et al.,<sup>23</sup> which includes 174 predicted ATP $\alpha$ 1 sequences from 161 insect species, with our alignment for firefly species (above). Considering all amino acid substitutions, naive to functional importance, we looked for those that 1) are present in at least 3 out of 7 *Photinus* species, 2) are not shared with direct outgroups, e.g., *Pyroactomena*, 3) are common in other CTS-associated species relative to other species. One site, and one substitution in particular (I787M) passes these filter criteria. I787M has independently evolved in five insect orders, and 6 out of 7 times it occurred in insects that either sequester or produce CTS ([Figure S5](#)).

### Differential expression analysis

*Photuris versicolor* females were fed with *Photinus pyralis* one day before dissection. RNA-seq data was generated as described in earlier sections. We created a modified *Photuris de novo* transcriptome reference by first identifying and removing any BLAST hits matching our reconstructed ATP $\alpha$ 1 sequences (BLAST 2.13.0+, with default parameters). In place of these, we added back full-length reconstructed ATP $\alpha$ 1 sequences. RNA-seq reads were mapped to this modified transcriptome reference using bwa mem (v 0.7.17)<sup>60</sup> and processed using SAMtools (v 1.15.1).<sup>56</sup> Counts were done by htseq-count (v 2.0.2, parameters: -a 0 -nonunique all). In order to use htseq-count, a gff3 file was made for our transcriptome with the perl script gmod\_fasta2gff3.pl ([key resources table](#)).

We used inverted beta-binomial (ibb) tests<sup>62P</sup> to determine the significance of difference of expression level among tissues and paralogs, and a standard Bonferroni correction was applied to account for multiple tests ([Table S2](#)). To visualize the differential expression among species, tissues, and paralogs, counts were normalized using the counts function (normalized=TRUE) of the R package DeSeq2.<sup>59</sup> Mekko chart was plotted using ggplot2 and mekko package implemented in R.

### CRISPR-cas9 engineered fly lines

For a list of all reagents used, see [Table S3](#). Details for each engineered fly line are as follows:

#### A119I

CRISPR-mediated mutagenesis of *D. melanogaster* was performed by WellGenetics using modified methods of Kondo and Ueda<sup>63</sup>: gRNA was designed and cloned into an expression vector containing a U6 promoter (pBFv-U6.2) and Cas-9 protein is supplied by a germline expression vector (pBFv-nosP-Cas9). ~1 kilobase homology arms were amplified using Phusion High-Fidelity DNA Polymerase (Thermo Scientific) from genomic DNA of the injection strain *w<sup>1118</sup>*. A plasmid donor template for repair, pUC57-Kan-A119I-pBacDsRed, was constructed containing 3xP3-DsRed and two homology arms flanked by pBac terminals ("TTAA"). The substitution A119I (standardized amino acid residue numbering) was introduced into ATP $\alpha$  coding sequence via point mutations changing the codon "GCC" to "ATC". Additional synonymous substitutions were added to eliminate three targeted PAM sites. For sequences of gRNA and homology arms. gRNA and donor plasmid constructs were confirmed by sequencing prior to injection. ATP $\alpha$ -targeting gRNAs and donor plasmid were microinjected into 210 embryos of the strain *w<sup>1118</sup>; attP40{nos-Cas9} / CyO*. Of 11 surviving G0

adults, 10 crosses to strain  $w^{[*];TM6B, Tb[1] / TM2, y+}$  were fertile and one was confirmed DsRed+. Insertion of the construct into the correct location was confirmed both by PCR and sequencing. *pBac-DsRed* was subsequently excised by first crossing to the strain  $w^{[*]; CyO, P\{Tub-pBac\} / Sp; +/TM6B}$  (Bloomington #8285) and subsequently to  $w^{[*]; TM3, Sb[1] Ser[1]/TM6B, Tb[1]}$  (Bloomington #2537). Repeated rounds of sib-mating were used to obtain stable homozygous lines. Precise excision of *pBacDsRed* and correctly-edited genome sequence was validated by genomic PCR and sequencing.

#### **Y108F-Q111E-A112S-S115L-E117T-A119N-D120N (“FESLTNN”)**

Engineered line Y108F-Q111E-A112S-S115L-E117T-A119N-D120N was generated by WellGenetics (Taipei, Taiwan) using the same methods as described for A119I (including the same homology arms and gRNA).  $222 w^{1118}; attP40\{nos-Cas9\}/CyO$  embryos were injected with the *ATP $\alpha$* -targeting gRNAs and donor plasmid. Of 18 surviving G0 adults, 15 were fertile in crosses to strain  $w^{[*];TM6B, Tb[1] / TM2, y+}$  and two were DsRed+. Both DsRed+ lines were PCR-sequence confirmed to contain correct insertions and processed to excise *pBac-DsRed* (as above). Each line was repeatedly sib-mated to generate homozygous lines and genome sequences were validated by genomic PCR and sequencing.

#### **Q111E-A112S-A119I-D120A (“ESIA”)**

Engineered line Q111E-A112S-A119I-D120A was generated by WellGenetics (Taipei, Taiwan) using the same methods as above (including homology arms and gRNA). Out of 645 microinjections of *ATP $\alpha$* -targeting gRNAs, a donor plasmid and a plasmid carrying *hsp70Bb-cas9* into  $w^{1118}$ , three lines were DsRed+ and validated carrying the correct insertion. However, after *pBac-DsRed* excision and repeated sib-mating, no homozygous mutant flies could be obtained. The bang sensitivity recovery time for ESIA/+ flies is 13.5 seconds ( $n=18$  flies), which is comparable to flies that are heterozygous for a *ATP $\alpha$ 1* loss-of-function mutation (i.e.  $\Delta 2-6b/+$ , Taverner et al.<sup>23</sup>; Figure 3). Thus, this is consistent with ESIA causing loss-of-function of the *D. melanogaster* *ATP $\alpha$ 1* protein (and not mutation to a secondary site that causes lethality).

#### **T797I**

Engineered line T797I was generated by WellGenetics (Taipei, Taiwan) using a unique gRNA and ~1kb homology arms. An additional mutation of a BsaI site GGTCTC → CGTCTC in the upstream homology arm in the donor plasmid was introduced to facilitate Golden Gate cloning. Of 422 injections of *ATP $\alpha$* -targeting gRNAs, two lines were DsRed+ and validated as carrying the correct insertion. However, after *pBac-DsRed* excision and repeated sib-mating, no homozygous mutant flies could be obtained for either line.

#### **F786Y and I787M**

Engineered lines F786Y and I787M were generated in-house with CRISPR-cas9 homology-dependent repair (HDR) using one gRNA and a template single-stranded donor oligonucleotide (ssODN). The designed gRNA showed no off-target sites by *in silico* prediction (using a web-based tool called “desktop”, which is now deprecated). Oligonucleotides (IDT) were annealed to generate a T7-gRNA expression template. This template was PCR amplified, size verified on a 2% agarose gel, purified using a QIAquick spin column (Qiagen), and eluted in 30  $\mu$ l Elution Buffer (Qiagen). *In vitro* transcription of gRNA templates was carried out by MEGAscript T7 Transcription Kit following the manufacturer’s protocol (Fisher Scientific). DNA and proteins were removed with turbo DNase and phenol:chloroform:isoamyl alcohol, respectively. RNA was purified with equal volume of isopropanol, washed twice with 70% ethanol, resuspended in 30  $\mu$ l RNase-free water, and quality checked on a Bioanalyzer (Agilent). Asymmetrical ssODN design was implemented to achieve better performance.<sup>64</sup> Synonymous mutations were introduced to facilitate downstream PCR screening. ssODNs were synthesized through IDT (Coralville, Iowa, USA)’s Ultramer DNA Oligo service. 20  $\mu$ l mixture of 100 ng/ $\mu$ l gRNA and 500 ng/ $\mu$ l ssODNs and Cas-9 mRNA were injected into 200 embryos of the line  $w^{1118}; attP40\{nos-Cas9\} / CyO$  by Rainbow Transgenic Flies (Camarillo, CA, USA). Approximately 5% of G0 offspring were fertile and were crossed to  $w^{[*]; TM3, Sb[1] Ser[1]/TM6B, Tb[1]}$  (Bloomington #2537). G1 flies were separated into individual vials and again crossed to the same double balancer line (Bloomington #2537). After 3-5 days, when enough eggs were laid, the genomic DNA of G1 flies was extracted using SquishPrep protocol. A 289-bp region spanning sites 786 and 787 was PCR-amplified with primers compatible with adding customized Illumina-style i5 and i7 indexes.<sup>21</sup> and paired-end 150 nt sequenced on Illumina MiSeq Nano (Genomics Core Facility, Princeton, NJ, USA). Three independent lines of F786Y and two lines of I787M were obtained and confirmed by sequencing. Progeny of G1 flies with the substitution F786Y or I787M were selected and sib-mated to obtain homozygous lines.

#### **Additional Lines Engineered Using the Method of Taverner et al.<sup>23</sup>**

Lines carrying Q111E, A112S, A119N, Q111E+A112S (“ES”) and Q111E+A112S+ A119N (“ESN”) were generated using the same method described in Taverner et al.<sup>23</sup> Substitutions, either individually or in combination, were engineered into the vector *pGX-attB-ATP $\alpha$ 42-6b* using Quick-change Lightning site-directed mutagenesis kit (Agilent). These plasmid constructs were injected into a white-eyed founder line  $w^{1118}; ATP\alpha 42-6b attP/TM6B, Tb1$  by Rainbow Transgenic Flies (Camarillo, CA, USA) following their standard protocol. Lines with successfully integrated constructs (i.e. indicated by red/pink eyes) were reduced with *cre-loxP* excision by crossing to  $y^1, w^{67c23}, P\{y[+mDint2]=Crey\}1b; D^*/TM3, Sb^1$  (Bloomington #851) and successfully reduced lines were balanced by crossing to  $w^*; ry^{506} Dr^1/TM6B, P\{w[+mC]=Dfd-EYFP\}3, Sb^1, Tb^1, ca^1$  (Bloomington 8704). Fluorescent offspring were sib-mated, and non-fluorescent *Tb*<sup>+</sup>, *Sb*<sup>+</sup> larvae were selected to generate stable homozygous lines. Substitutions were validated by PCR and sequencing.

#### **CTS tolerance assay**

Fireflies are protected by lucibufagins, a class of cardiotonic steroids (“CTS”). To measure the tolerance of engineered fly lines to CTS exposure, we introduced adult flies to food media containing varying concentrations of the representative CTS ouabain (ouabain

octahydrate, Sigma-Aldrich, Cat# O-3125) and recorded how many of adults survived after 7 days. We used 0.7 grams of dried instant media (Flystuff (66-117) Nutri-fly Instant) reconstituted in a standard fly vial with 3.5 ml of 0, 5, 10, 15, or 20 mM ouabain solutions. Although the physiologically relevant concentrations of lucibufagins in fireflies are unknown, a previous study showed that wild-type flies exhibited high fatality rates upon exposure to 5 mM ouabain.<sup>23</sup> Reconstituted food was allowed to set for 30 minutes, and a small piece of Kimwipe tissue was added to absorb the moisture. 10 male and 10 female flies that had enclosed within 7 days were placed in each vial (three replicates per line and concentration), and kept at 25°C, 50% humidity for 7 days. Mortality rate was measured by counting the number of living flies after 7 days. Mortality was not sex-dependent, as expected based on a previous study.<sup>23</sup> The Cochran-Mantel-Haenzel test implemented in R was used to assess significant differences between ouabain treatments (5/10/15/20 mM) versus no ouabain.

### Enzyme inhibition assays

CTS inhibit the ATPase activity of NKA. The principle of enzyme inhibition assays is to determine the ATPase activity of NKA by photo-metrically measuring the phosphate released from ATP during enzymatic hydrolysis at various concentrations of CTS. These assays were performed on wild-caught fireflies, soldier beetles and on engineered fly lines. All samples were stored at -80°C to minimize protein degradation. After thawing, fireflies and soldier beetles were immersed in deionized water and nervous tissue (brains and ventral nerve cords) was dissected under a stereomicroscope. 10 and 20 *Photinus*, 4 or 7 *Photuris*, or 10 *Rhagonycha* were pooled into each biological replicate. For flies, 90 heads were pooled together for each biological replicate (two biological replicates for *Photinus* and three for *Photuris*, *Rhagonycha* and *Drosophila*). Samples were prepared and the activities of NKA were measured following the procedures described in Taverner et al.<sup>23</sup> Tissues were suspended and homogenized in deionized water using a glass grinder (Wheaton) on ice. Homogenates (split into three technical replicates for *Drosophila*), were freeze-dried (Christ, Alpha 2-4 LDPlus) overnight, and lyophilisates were reconstituted immediately before use. Samples were incubated in 6 (for beetles) or 12 (for *Drosophila*) increasing concentrations of ouabain (100 mM NaCl, 20 mM KCl, 4 mM MgCl<sub>2</sub>, 50 mM imidazol, and 2.5 mM ATP) at 37 °C for 20 minutes. A non-inhibited positive control was carried out without the addition of ouabain, and the negative control was deprived of KCl and incubated at 2 × 10<sup>-3</sup> M both ouabain (inactive NKA) for complete inhibition of NKA to correct for background phosphate. Absorbance was measured at 700 nm on a CLARIOstar microplate reader (BMG Labtech, Germany). For *Drosophila*, each biological replicate was averaged over three technical replicates. Due to the limited availability of material, no technical replicates were carried out for beetle NKAs.

Relative activities of NKA were estimated for each ouabain concentration as (abs[full activity]-abs[inhibited activity])/(abs[full activity]-abs[background activity]). Curve fitting was performed with the nlsLM function from the minipack.lm library in R using the function

$$\text{Relative Activity} = \frac{1}{(1+10^{-IC50+x})^{*hs}}$$

where,  $x$  is the ouabain concentration,  $IC50$  is the ouabain concentration corresponding to 50% relative activity, and  $hs$  is the slope coefficient. Approximate 95% confidence intervals for  $IC50$  were estimated by parametric bootstrapping as described in Taverner et al.<sup>23</sup> (Table S4).

For *Photuris versicolor*, the inhibition curve does not appear to be monophasic since relative enzyme activity is still ~40% at the highest ouabain concentration. We thus made some simplifying assumptions to estimate approximate  $IC50$ s. First, it was assumed that the curve is biphasic, reflecting activities of primarily two enzyme isoforms. This can be justified by the fact that in nervous tissue (from which enzyme preps were made), paralogs ATP $\alpha$ 1A and ATP $\alpha$ 1C are roughly equally expressed and together account for ~90% of total ATP $\alpha$  expression (Figure 2C). We thus used the equation

$$\text{Relative Activity} = \frac{(1-f)}{(1+10^{-IC50_1+x})} + \frac{f}{(1+10^{-IC50_2+x})}$$

where,  $x$  is the ouabain concentration,  $IC50_1$  and  $IC50_2$  are the ouabain concentration corresponding to 50% relative activity for each isoform, respectively,  $f$  is the total activity attributable to the second isoform and  $hs$  for both enzyme isoforms is assumed to be ~1. Approximate 95% confidence intervals for  $IC50_1$  and  $IC50_2$  were estimated by parametric bootstrapping as above.

### Bang-sensitivity assay

The “bang-sensitivity” assay is a classical test where mutants with defective neurological functions experience seizures and paralysis upon mechanical over-stimulation.<sup>23,24,36,65</sup> Individual 14-day old male flies were placed in an empty *Drosophila* vial, vortexed at the maximum speed for 20 seconds, and immediately dumped to a surface. The time required for each individual to right itself was recorded (times >120 seconds were pooled into one timepoint). 30-50 flies were tested for each genotype. One engineered strain, ESN, was assayed in fewer individuals due to the poor condition of the flies.

### QUANTIFICATION AND STATISTICAL ANALYSIS

To determine the difference of expression level of NKA among tissues and paralogs, we used the beta-binomial (ibb) test<sup>62</sup> followed by a standard Bonferroni correction. Statistical tests are summarized in Table S2. To evaluate differences in adult tolerance to CTS

exposure, the Cochran-Mantel-Haenzel test implemented in R was used to assess significant differences between ouabain treatments (5/10/15/20 mM) versus no ouabain. We used 3 replicates (20 individuals each) per line per condition. Mean and standard errors are represented [Figures 3](#) and [4](#). To determine the relative activities of NKA for each ouabain concentration, 95% confidence intervals of IC50 were estimated by parametric bootstrapping as described in Taverner et al.<sup>23</sup> Estimated parameters can be found in [Table S4](#). Number of biological replicates used is indicated in the legends of [Figures 1](#), [3](#), and [4](#). For bang-sensitivity assays, 30-50 individuals were tested for each genotype. Mean and standard errors are represented in [Figures 3](#) and [4](#).